The Journal of Experimental Medicine

Targeting Platelet–Leukocyte Interactions: Identification of the Integrin Mac-1 Binding Site for the Platelet Counter Receptor Glycoprotein Ibα

Raila Ehlers,[1] Valentin Ustinov,[3] Zhiping Chen,[1] Xiaobin Zhang,[1] Ravi Rao,[2] F. William Luscinskas,[2] Jose Lopez,[4] Edward Plow,[3] and Daniel I. Simon[1]

[1]*Cardiovascular Division and* [2]*Department of Pathology, Brigham and Women's Hospital, Boston, MA 02115*
[3]*The Cleveland Clinic Foundation, Cleveland, OH 44195*
[4]*Thrombosis Research Section, Departments of Medicine and Molecular and Human Genetics, Baylor College of Medicine, Houston, TX 77030*

Abstract

The firm adhesion and transplatelet migration of leukocytes on vascular thrombus are dependent on the interaction of the leukocyte integrin Mac-1 ($\alpha_M\beta_2$, CD11b/CD18) and the platelet counter receptor glycoprotein (GP) Ibα. Previous studies have established a central role for the I domain, a stretch of ~200 amino acids within the α_M subunit, in the binding of GP Ibα. This study was undertaken to establish the molecular basis of GP Ibα recognition by $\alpha_M\beta_2$. The P^{201}–K^{217} sequence, which spans an exposed loop and amphipathic α4 helix in the three-dimensional structure of the α_MI domain, was identified as the binding site for GP Ibα. Mutant cell lines in which the α_MI domain segments P^{201}–G^{207} and R^{208}–K^{217} were switched to the homologous, but non-GP Ibα binding, α_L domain segments failed to support adhesion to GP Ibα. Mutation of amino acid residues within P^{201}–K^{217}, H^{210}–A^{212}, T^{213}–I^{215}, and R^{216}–K^{217} resulted in the loss of the binding function of the recombinant α_MI domains to GP Ibα. Synthetic peptides duplicating the P^{201}–K^{217}, but not scrambled versions, directly bound GP Ibα and inhibited $\alpha_M\beta_2$-dependent adhesion to GP Ibα and adherent platelets. Finally, grafting critical amino acids within the P^{201}–K^{217} sequence onto α_L, converted $\alpha_L\beta_2$ into a GP Ibα binding integrin. Thus, the P^{201}–K^{217} sequence within the α_MI domain is necessary and sufficient for GP Ibα binding. These observations provide a molecular target for disrupting leukocyte–platelet complexes that promote vascular inflammation in thrombosis, atherosclerosis, and angioplasty-related restenosis.

Key words: inflammation • leukocytes • platelets • adhesion • receptors

Introduction

Adhesive interactions between vascular cells play important roles in orchestrating the inflammatory response. Recruitment of circulating leukocytes to vascular endothelium requires multistep adhesive and signaling events, including selectin-mediated attachment and rolling, leukocyte activation, and integrin-mediated firm adhesion and diapedesis that result in the infiltration of inflammatory cells into the blood vessel wall (1). Firm attachment is mediated by members of the β_2 integrin family, LFA-1 ($\alpha_L\beta_2$, CD11a/CD18), Mac-1 ($\alpha_M\beta_2$, CD11b/CD18), and p150,95 ($\alpha_M\beta_2$, CD11c/CD18), which bind to endothelial counter ligands (e.g., intercellular adhesion molecule [ICAM]-1; 2), endothelial-associated extracellular matrix proteins (e.g., fibrinogen; 3), or glycosaminoglycans (4).

Leukocyte recruitment and infiltration also occur at sites of vascular injury where the lining endothelial cells have been denuded and platelets and fibrin have been deposited.

R. Ehlers and V. Ustinov contributed equally to this work.

Address correspondence to Daniel I. Simon, Brigham and Women's Hospital, Cardiovascular Division, 75 Francis Street, Tower 3, Boston, MA 02115. Phone: (617) 732-5867; Fax: (617) 732-5132; email: dsimon@rics.bwh.harvard.edu

Abbreviations used in this paper: BCECF AM, 2′,7′-bis-(2-carboxyethyl)-5-(and-6)-carboxyfluorescein, acetoxymethyl ester; GP, glycoprotein; GST, glutathione *S*-transferase; ICAM, intercellular adhesion molecule; MFI, mean fluorescence intensity; NIF, neutrophil inhibitory factor; RU, resonance unit; sGP Ibα, soluble extracellular region of GP Ibα (i.e., glycocalicin); vWf, von Willebrand factor.

 J. Exp. Med. © The Rockefeller University Press • 0022-1007/2003/10/1077/12 $8.00
Volume 198, Number 7, October 6, 2003 1077–1088
http://www.jem.org/cgi/doi/10.1084/jem.20022181

A similar sequential adhesion model of leukocyte attachment to and transmigration across surface-adherent platelets has been proposed (5). The initial tethering and rolling of leukocytes on platelet P-selectin (6) are followed by their firm adhesion and transplatelet migration, processes that are dependent on $\alpha_M\beta_2$ (5).

Our laboratory has focused on identifying the platelet counter receptor for $\alpha_M\beta_2$. Evaluation of the structural features of integrins provides insight into candidate platelet counter receptors for $\alpha_M\beta_2$. Integrins are heterodimeric proteins composed of one α and one β subunit. A subset of integrin α subunits, including α_M, contains an inserted domain (I domain) of ~200 amino acids that is implicated in ligand binding (7–9) and strikingly similar to the A domains of von Willebrand factor (vWf; 10), one of which, A1, mediates the interaction of vWf with its platelet receptor, the glycoprotein (GP) Ib-IX-V complex. Because of the similarity of the vWf A1 domain and the α_MI domain, we hypothesized that GP Ibα might also be able to bind $\alpha_M\beta_2$ and reported that GP Ibα is indeed a constitutively expressed counter receptor for $\alpha_M\beta_2$ (11). Furthermore, under the conditions used in these studies, the predominant interaction between neutrophils and platelets appeared to be between $\alpha_M\beta_2$ and GP Ibα (11).

The α_MI domain contributes broadly to the recognition of ligands by $\alpha_M\beta_2$ (12) and specifically to the binding of GP Ibα (11). This region has been implicated in the binding of ICAM-1 (13), iC3b (14), fibrinogen (12, 13), and neutrophil inhibitory factor (NIF; 15), as well as GP Ibα. Previous studies suggested that overlapping, but not identical, sites are involved in the recognition of iC3b, fibrinogen, and NIF (16, 17). Although the binding sites for iC3b, NIF, and fibrinogen in the α_MI domain have been mapped extensively (18–23), the recognition site for GP Ibα is unknown.

In this study, we have localized the binding site for GP Ibα within the α_MI domain. The strategy developed was based on the differences in the binding of GP Ibα to the α_MI and α_LI domains and involved several independent approaches, including screening of mutant cells, synthetic peptides, site-directed mutagenesis, and gain in function analyses. The binding site for GP Ibα was localized within the segment $\alpha_M(P^{201}–K^{217})$. The grafting of two amino acids within this segment into the α_LI domain converted it to a GP Ibα–binding protein. Thus, a small segment that has a defined structure within the α_MI domain is necessary and sufficient for GP Ibα binding.

Materials and Methods

Materials. The soluble extracellular region of GP Ibα (sGP Ibα; i.e., glycocalicin) was purified as we previously reported (11). Human fibrinogen depleted of plasminogen, vWf, and fibronectin was purchased from Enzyme Research Laboratories.

The CD11/CD18 mAbs used included the following: LPM19c, directed to the α_MI domain (provided by K. Pulford, Radcliffe, Oxford, United Kingdom; 12); OKM1, directed to the α_M subunit of human Mac-1 (American Type Culture Collection [ATCC]); M1/70, directed to the α_M subunit mouse $\alpha_M\beta_2$ (ATCC; 24); CBRM1/5, an activation-specific α_M reporter antibody (provided by T. Springer, Harvard Medical School, Boston, MA; 25); TS1/22, directed to the α_L subunit of $\alpha_L\beta_2$ and capable of blocking ICAM-1 binding (ATCC); MEM-83, an activation-specific α_L reporter antibody (Caltag); and IB4, a blocking mAb directed to the β_2 subunit (ATCC). The stimulating CD18 mAb KIM127 (26) was provided by M. Robinson (Celltech Ltd., Slough, United Kingdom). mAb24, a β_2 activation reporter antibody (27), was provided by N. Hogg (Imperial Cancer Research Fund, Lincoln's Inn Fields, London, United Kingdom).

Peptides were obtained from the W.M. Keck Biotechnology Resource Center at Yale University. The peptides were diluted in DMSO and stored at −80°C.

Cell Lines and Culture Conditions. THP-1 monocytic cells (ATCC) were maintained and differentiated with 1 ng/ml TGF-β1 and 50 nM 1,25-$(OH)_2$ vitamin D3, as previously described (28). 293 cells expressing human $\alpha_L\beta_2$, $\alpha_M\beta_2$, or mutant $\alpha_M\beta_2$ receptors were established and maintained as previously described (16, 20, 23, 29).

Segment Switches by Site-directed Mutagenesis. To systematically define the GP Ibα–binding site in α_M, a homologue-scanning mutagenesis strategy was implemented (20). Accordingly, guided by the crystal structure (8, 9), the hydrated surface of the α_MI domain was replaced with sequences of the α_LI domain in segments of 7–11 amino acids. To apply this approach to the α_MI domain (~200 amino acids), 16 segments were switched (20, 23). Site-directed mutagenesis of the α_MI domain was performed using QuikChange Site-Directed Mutagenesis Kit (Stratagene). The mutations introduced and the mutagenic primers used have been reported (23). The appropriate DNA sequence of the entire I domain (from I^{139} to A^{332}) was confirmed for each mutant before transferring back into the α_M subunit cDNA.

Transient Transfection. The expression vector pcDNA3.1 (Invitrogen) was used for cloning α_M, α_L, and β_2 from human leukocyte cDNA library. 293 cells were transfected using the Lipofectamine 2000 reagent (Invitrogen) with 24 μg DNA/vessel for 4 h, according to the manufacturer's instructions. After transfection, the medium was replaced with full growth medium. The functional assays were prepared 48 h after transfection.

Flow Cytometry. FACS® analyses were performed to assess the expression of wild-type and mutated forms of $\alpha_M\beta_2$ and $\alpha_L\beta_2$ on the surface of transfected 293 cells, as previously described (11). Platelet P-selectin expression was assessed using FITC-conjugated AK-4 or isotype control (BD Biosciences).

Preparation of Neutrophils and Platelets. Neutrophils from wild-type (Mac-$1^{+/+}$) and Mac-1–deficient (Mac-$1^{-/-}$; 30) C57Bl/J6 mice were harvested and purified from the peritoneal cavity after the intraperitoneal injection of 1 ml sterile 3% thioglycollate broth, as previously described (11).

Venous blood was obtained from volunteers who had not consumed aspirin or other nonsteroidal antiinflammatory drugs for at least 10 d and was anticoagulated with 13 mM trisodium citrate, which also contained 100 nM prostaglandin E_1. Platelet-rich plasma was prepared by centrifugation at 150 *g* for 10 min. Gel-filtered platelets were obtained by passage of platelet-rich plasma over a Sepharose-2B column in calcium-free Tyrode's-Hepes buffer containing 100 nM prostaglandin E_1, as previously described (11).

Adhesion Assays. Adherent cells were assayed by loading 293 cells and thioglycollate-elicited murine neutrophils with 1 μM 2′,7′-bis-(2-carboxyethyl)-5-(and-6)-carboxyfluorescein, acetoxymethyl ester (BCECF AM), according to the manufacturer's instructions (Molecular Probes). 10^5 cells/well were placed in 96-

well microtiter plates coated with 10 μg/ml sGP Ibα or 10 μg/ml fibrinogen and blocked with 0.2% gelatin. Adhesion was stimulated with 20 ng/ml PMA or 5 μg/ml of the β2-stimulating mAb KIM 127. Plates were washed and adhesion was quantified by measuring the fluorescence of BCECF AM–loaded cells using a Cytofluor II fluorescence microplate reader (PerSeptive Biosystems). The effect of anti-α_M mAb on adhesion was assessed by preincubating cells with 10 μg/ml LPM19c. The effect of peptides M1–M8 on adhesion was investigated by incubating the indicated peptide with sGP Ibα–coated wells for 30 min at 37°C before the addition of cells. Data are expressed as percent adhesion of control treatment.

Neutrophil Adhesion to Surface-adherent Platelets. Neutrophil adhesion to surface-adherent platelets was investigated as previously described (11). The effect of α_M peptides on leukocyte adhesion to platelets was examined by preincubating surface-adherent platelets with peptide (1–1,000 nM) or vehicle for 30 min at 37°C. Data are expressed as percent adhesion of control treatment.

Site-directed Mutagenesis, Expression, and Purification of I Domain Fusion Proteins. The cDNAs of α_MI domain (675 nucleotides, R^{115}–S^{340}), α_LI domain (630 nucleotides, P^{120}–S^{330}), and mouse α_MI domain (675 nucleotides, L^{115}–S^{340}) were cloned and inserted into the pGEX-5X-3 expression vector (22). All wild-type and mutant I domains were expressed as glutathione *S*-transferase (GST) fusion proteins. Mutations were created in these I domains and intact α_L by oligonucleotide-directed mutagenesis. The selective introduction of the desired mutations into the I domains was confirmed by DNA sequence analyses. The GST-I domain fusion proteins were purified by adsorption onto glutathione-Sepharose 4B (Amersham Biosciences) and eluted with buffer containing 50 mM Tris-HCl, pH 8.0, 150 mM NaCl, 5 mM glutathione, 2.5 mM $CaCl_2$. Such preparations of the fusion proteins were ~90% pure as assessed by SDS-PAGE.

GP Ibα Binding to the I Domains. To test the interaction of the wild-type α_M, α_L, and chimeric I domains with biotinylated GP Ibα, 96-well plates (Immulon 4BX; Dynex Technologies Inc.) were coated with the I domains at 50 μg/ml and blocked with 2% BSA. sGP Ibα in 20 mM Tris-HCl, pH 7.6, containing 100 mM NaCl and 2 mM $CaCl_2$, was added to the wells and incubated for 1 h at 37°C. After washing, bound GP Ibα was detected using avidin-alkaline phosphatase and *p*-nitrophenyl phosphate. Background reaction on BSA-coated wells was subtracted.

BIAcore Surface Plasmon Resonance Analysis. Real-time protein–protein interactions were examined using surface plasmon resonance on a BIAcore 1000 (BIAcore AB). Immobilization of peptides was performed via thiol coupling onto a sensor chip C1 using 20 mM Tris, 150 mM NaCl, 2 mM $MgCl_2$, pH 7.4, as running buffer at a flow rate of 5 μl min^{-1}. Modified versions of peptides containing an amino-terminal cysteine residue were synthesized and then diluted in10 nM acetate buffer, pH 5.0 (coupling buffer). The peptide was loaded on the chip for 16 min and immobilization occurred via thiol disulfide exchange. Identical treatment was applied to the reference flow cell without peptide (control surface). For analysis, sGP Ibα diluted into running buffer was injected at a flow rate of 10 μl/min. Binding (resonance unit [RU]) was measured as a function of time(s). Binding data (after subtracting nonspecific background binding to the control surface) are presented as sensorgrams, binding curves, and Scatchard plots (31).

In Vitro Analysis of Cellular Adhesion under Laminar Flow Conditions. The laminar flow chamber used in this assay has been described (32). 25 mm^2 diameter glass coverslips (Assistent; Carolina Biological Supply Company) were coated with a solution of 20 μg/ml soluble P-selectin (provided by R. Camphausen, Genetics Institute, Cambridge, MA) and 40 μg/ml sGP Ibα for 2 h at room temperature. Nonspecific interactions were blocked with PBS containing 1% human serum albumin for 1 h at room temperature and with 0.1% Tween 20 immediately before use. The effect of M2 and scM2 peptides on THP-1 cell rolling and firm arrest was examined by incubating 50 μM of the peptide with the ligand-coated glass coverslip for 1 h at room temperature. To block PSGL-1 and $\alpha_M\beta_2$ interactions, THP-1 cells were incubated with 20 μg/ml KPL-1 (BD Biosciences) or 20 μg/ml LPM19c mAb, respectively, for 20 min before perfusion. $\alpha_M\beta_2$ was activated by treating cells with 10 μg/ml KIM127 for 5 min before perfusion. The rolling and firm adhesive events scored were ligand specific as confirmed in parallel determinations on control substrates coated with human serum albumin. Coverslips were inserted in the flow chamber and 0.6×10^6/ml THP-1 cells were drawn across at an estimated shear stress of 0.75 dynes/cm^2 using a syringe pump (Harvard Apparatus). After 3 min of perfusion, the number of rolling and arrested cells was quantified in each of five random 10x fields (area ~0.3 mm^2) by an investigator blinded to treatment.

Statistics. Data are presented as the mean ± SD or SEM. Groups were compared using the nonpaired *t* test. Rolling and arrest data were analyzed using repeated measure ANOVA with a Bonferroni corrective for multiple comparisons. P values <0.05 were considered significant.

Results

Binding of GP Ibα to Mutant Cell Lines. Our previous report indicated that the α_MI domain serves as a recognition site for GP Ibα (11). The adhesion of $\alpha_M\beta_2$-bearing cells to sGP Ibα was inhibited by LPM19c, an mAb that binds to the α_MI domain. To establish definitively that the α_MI domain serves as a recognition site for GP Ibα, we transfected 293 cells with wild-type $\alpha_M\beta_2$, $\alpha_L\beta_2$, or a chimeric $\alpha_L\beta_2$ receptor that contained the I domain of $\alpha_M\beta_2$ (i.e., $\alpha_L(I\alpha_M)\beta_2$-transfected 293 cells). $\alpha_L\beta_2$-transfected 293 cells did not adhere to sGP Ibα. In contrast, $\alpha_L(I\alpha_M)\beta_2$-transfected 293 cells adhered robustly to sGP Ibα in a manner similar to $\alpha_M\beta_2$-transfected 293 cells, indicating that the α_MI domain is required for adhesion to sGP Ibα. These data suggest that although $\alpha_M\beta_2$ and $\alpha_L\beta_2$ are highly homologous integrins, the lack of binding of sGP Ibα to $\alpha_L\beta_2$ might be the result of sequence and/or structural differences.

As the first step to define the binding site for GP Ibα within the α_MI domain, mutant cell lines, each expressing a mutant $\alpha_M\beta_2$ in which a short α_MI domain sequence, corresponding to a structural unit in the crystal structure (8, 9), was replaced for the corresponding region of the α_LI domain, were tested for their adhesion to immobilized sGP Ibα. 16 segments were switched from their original α_MI domain to their counterparts in α_L (16, 20, 23). These segment swaps are placed throughout the P^{147}–Q^{314} region of the α_MI domain, D^{132}–A^{318}, and are intended to cover its entire hydrated surface (8, 9). For such experiments to be readily interpretable, cell lines expressing high and similar levels of wild-type and mutant receptors were selected by cell sorting using mAbs OKM1 and IB4 followed by cloning by limiting dilution. The expression of the receptors as assessed by the mean fluorescence intensity (MFI) in

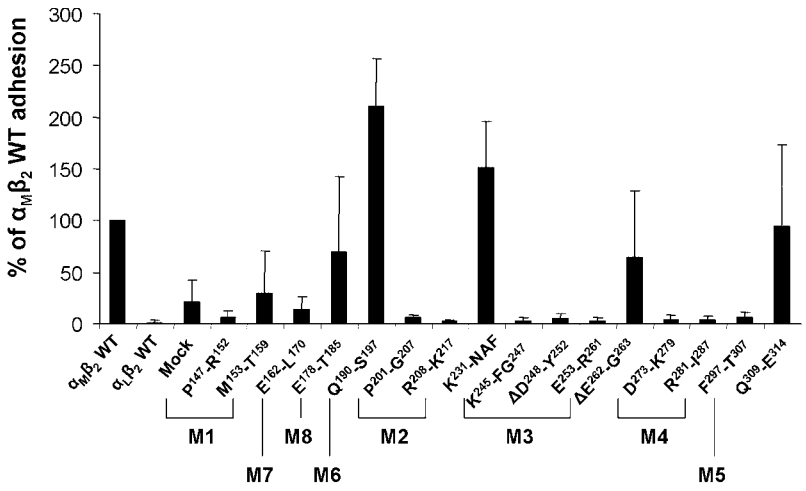

Figure 1. Binding of GP Ibα to mutant cell lines. Adhesion of 10^5 $\alpha_M\beta_2$-, $\alpha_L\beta_2$-, and mutant $\alpha_M\beta_2$-expressing 293 cells to sGP Ibα–coated wells. Adhesion was promoted by the addition of 5 μg/ml of the stimulating mAb KIM 127 and quantified by measuring the fluorescence of BCECF AM–loaded cells. Data are expressed as percent wild-type $\alpha_M\beta_2$ adhesion (mean ± SD of three to five independent experiments). A series of peptides (M1–M8) corresponding to the wild-type α_MI domain sequences were synthesized and tested for their ability to interact with sGP Ibα (Table I). Because the sequences within several of the negative mutants were contiguous, linear peptides spanning these sequences were synthesized: P^{147}–T^{159} (M1), P^{201}–K^{217} (M2), K^{245}–R^{261} (M3), D^{273}–I^{287} (M4), F^{297}–T^{307} (M5), Q^{190}–S^{197} (M6), E^{162}–L^{170} (M7), and E^{178}–T^{185} (M8). All peptides correspond to negative mutant sequences except M6 and M8, which correspond to intermediate and positive mutant sequences, respectively.

FACS® analyses differed by less than twofold from the internal wild-type control (not depicted).

The results of adhesion of 16 mutants to sGP Ibα are summarized in Fig. 1. The data are expressed as the percent adhesion of the wild-type $\alpha_M\beta_2$-expressing cells to sGP Ibα. Substitutions for the following regions of α_MI domain abrogated adhesion: $\alpha_M(P^{147}$–$R^{152})$, $\alpha_M(M^{153}$–$T^{159})$, $\alpha_M(E^{162}$–$L^{170})$, $\alpha_M(P^{201}$–$G^{207})$, $\alpha_M(R^{208}$–$K^{217})$, $\alpha_M(K^{245}FG^{247})$, $\alpha_M(\Delta D^{248}$–$Y^{252})$, $\alpha_M(E^{253}$–$R^{261})$, $\alpha_M(D^{273}$–$K^{279})$, $\alpha_M(R^{281}$–$I^{287})$, and $\alpha_M(F^{297}$–$T^{307})$. These cell lines form a group of negative mutants. As the essential control, the $\alpha_L\beta_2$-expressing cells adhered poorly to sGP Ibα, consistent with lack of interaction of $\alpha_L\beta_2$ with sGP Ibα.

The lack of adhesion of these mutants was not the result of decreased surface expression of the receptor because there was no correlation between the level of adhesion and expression. Specifically, surface expression of the $\alpha_M(P^{201}$–$G^{207})$ mutant was 1.5-fold higher than that of the cells expressing the wild-type $\alpha_M\beta_2$ cells, but adhesion was abrogated completely. Surface expression of negative mutants, $\alpha_M(P^{147}$–$R^{152})$, $\alpha_M(R^{208}$–$K^{217})$, $\alpha_M(E^{253}$–$R^{261})$, and $\alpha_M(D^{273}$–$K^{279})$ was very similar to that of the wild-type receptor. Adhesion of $\alpha_M(E^{178}$–$T^{185})$ and $\Delta E^{262}G^{263}$ was partially affected. The maximal level of adhesion to sGP Ibα reached 69 and 64%, respectively, of wild-type $\alpha_M\beta_2$ cells. These two receptors were classified as intermediate mutants.

The following mutants supported the same or higher levels of adhesion to sGP Ibα compared with the cells expressing the wild-type $\alpha_M\beta_2$ receptor: $\alpha_M(Q^{190}$–$S^{197})$, $\alpha_M(K^{231}NAF^{234})$, $\alpha_M(E^{262}$–$G^{263})$, and $\alpha_M(Q^{309}$–$E^{314})$. The cell lines exhibiting adhesion similar to or greater than the wild-type $\alpha_M\beta_2$ cells were identified as positive mutants. Two of these positive mutants, $\alpha_M(Q^{190}$–$S^{197})$ and $\alpha_M(K^{231}NAF^{234})$, bound sGP Ibα better than wild-type $\alpha_M\beta_2$. Previous analyses using these mutants showed that they bound neither an $\alpha_M\beta_2$ activation-independent ligand, NIF (20), nor $\alpha_M\beta_2$ activation-dependent ligands, C3bi (17) and fibrinogen (23), to a greater extent than wild-type receptor. Thus, the enhanced binding of these mutants appears to be selective for sGP Ibα recognition. In further studies, we found that binding of the β_2 activation–specific reporter mAb 24 was similar for wild-type and the α_M $(Q^{190}$–$S^{197})$ and $\alpha_M(K^{231}NAF^{234})$ mutants. In contrast, increased binding of the α_M activation–specific reporter CBRM1/5 to $\alpha_M(K^{231}NAF^{234})$ compared with wild-type $\alpha_M\beta_2$ and $\alpha_M(Q^{190}$–$S^{197})$ suggests possible conformation change of the $\alpha_M(K^{231}NAF^{234})$ mutant (not depicted). Together, these observations suggest that the activation states of $\alpha_M\beta_2$ may reflect the reporter ligand or mAb used, and these two mutants might be functionally activated with respect to sGP Ibα recognition.

Interaction of GP Ibα with the α_MI Domain Peptides. In subsequent analyses, we focused on the 11 negative mutants. A series of peptides (M1–M8) corresponding to the wild-type α_MI domain sequences were synthesized and tested for their ability to interact with sGP Ibα. Because the sequences within several of the negative mutants were contiguous, the following linear peptides spanning these sequences were synthesized: P^{147}–T^{159} (designated M1), P^{201}–K^{217} (M2), K^{245}–R^{261} (M3), D^{273}–I^{287} (M4), F^{297}–T^{307} (M5), Q^{190}–S^{197} (M6), E^{162}–L^{170} (M7), and E^{178}–T^{185} (M8). All peptides correspond to negative mutant sequences except M6 and M8, which correspond to intermediate and positive mutant sequences, respectively.

Next, we examined the effect of these α_MI domain peptides on $\alpha_M\beta_2$-dependent adhesion to sGP Ibα or fibrinogen (Table I). 50 μM peptides were preincubated in ligand-coated wells, $\alpha_M\beta_2$-expressing 293 cells were added, and adhesion was stimulated with KIM 127. Mac-1 293 cells adhered to sGP Ibα and fibrinogen, and this adhesion was blocked by the anti-CD11b mAb LPM19c, indicating that adhesion is predominantly $\alpha_M\beta_2$ dependent (Table I). Peptide M2 inhibited adhesion to sGP Ibα (percent inhibition = 74 ± 13; $P < 0.01$). Interestingly, M2 had no effect on cellular adhesion to fibrinogen. All other peptides had minimal or no effect on $\alpha_M\beta_2$-expressing 293 cell adhesion to sGP Ibα or fibrinogen. M2, but not a scrambled version (scM2), blocked $\alpha_M\beta_2$-dependent adhesion to sGP Ibα in a dose-dependent manner (IC_{50} = 20 μM; Fig. 2). Taken together, these observations suggest that the α_MI domain se-

Table I. *Effect of $\alpha_M I$ Domain Peptides on $\alpha_M\beta_2$ 293 Cell Adhesion to sGP Ibα and Fibrinogen*

Peptide or mAb	α_MI domain sequence	Peptide sequence	Percent $\alpha_M\beta_2$ 293 adhesion to sGP Ibα	Percent $\alpha_M\beta_2$ 293 adhesion to fibrinogen
M1	P^{147}–T^{159}	PHDFRRMKEFVST	76 ± 18	118 ± 27
M2	P^{201}–K^{217}	PITQLLGRTHTATGIRK	26 ± 13[a]	102 ± 46
M3	K^{245}–R^{261}	KFGDPLGYEDVIPEADR	94 ± 20	136 ± 32
M4	D^{273}–I^{287}	DAFRSEKSRQELNTI	110 ± 36	115 ± 8
M5	F^{297}–T^{307}	FQVNNFEALKT	96 ± 16	105 ± 12
M6	Q^{190}–S^{197}	QNNPNPRS	93 ± 17	107 ± 3
M7	E^{162}–L^{170}	EQLKKSKTL	79 ± 31	103 ± 3
M8	E^{178}–T^{185}	EEFRIHFT	66 ± 27	104 ± 11
C-M2	P^{201}–K^{217}	CPITQLLGRTHTATGIRK	26 ± 1[a]	ND
scM2		LGTRITHQRTGPTIKL	80 ± 15	ND
LPM19c	Anti-α_MI domain		6.3 ± 5.7[b]	6.1 ± 6.6[b]

The adhesion of $\alpha_M\beta_2$-expressing 293 cells to sGP Ibα– or fibrinogen-coated microtiter wells was stimulated by the addition of 5 μg/ml KIM 127 in the presence and absence of 50 μM α_MI domain peptides or 10 μg/ml antibody (LPM19c). Data are expressed as percent adhesion with vehicle alone. Mean ± SD, n = 3–5.
[a]$P < 0.01$.
[b]$P < 0.0001$.

quence corresponding to M2 (P^{201}–K^{217}), which spans an exposed loop and amphipathic α4 helix in the three-dimensional structure of the α_MI domain, contributes to $\alpha_M\beta_2$ binding of GP Ibα.

Real-Time Detection of Protein–Protein Interaction by BIAcore Analyses Reveals Specific, Direct Binding of GP Ibα to M2 Peptide. To examine direct interactions between GP Ibα and M2, we used an in vitro real-time binding assay using surface plasmon resonance (BIAcore). M2 and scM2 peptides were modified by addition of an amino-terminal cysteine and immobilized via thiol coupling on a C1 sensor chip. Cys-M2, but not Cys-scM2, inhibited $\alpha_M\beta_2$-dependent adhesion to sGP Ibα, verifying that cysteine addition did not adversely affect peptide structure (Table I). Increasing concentrations of purified sGP Ibα in running buffer containing 2 mM $MgCl_2$ were injected over the chip surface and the sensorgrams were recorded. As shown in Fig. 3, the sensorgrams detected little interaction between sGP Ibα and control chips or chips containing immobilized scM2. Significant interaction responses were detected for sGP Ibα with M2. Apparent equilibrium dissociation constant was estimated from the equilibrium resonance signal as a function of analyte (GP Ibα) concentration (kD ~20 μM) and calculated by Scatchard analysis (kD = 17 μM). Similar results were obtained when purified sGP Ibα in running buffer containing 2 mM $CaCl_2$ were injected over the chip surface (not depicted). Thus, BIAcore analysis revealed real-time, direct binding for bimolecular interactions between GP Ibα and M2.

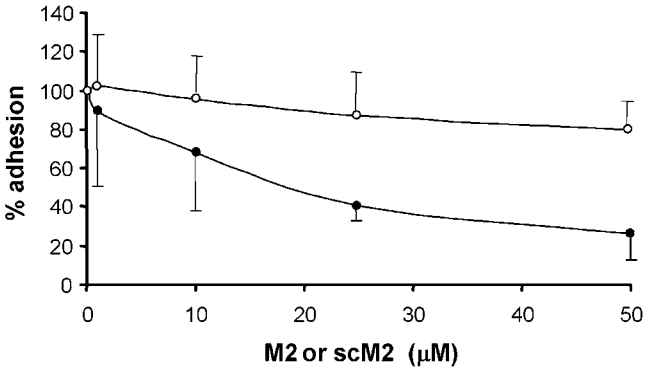

Figure 2. Effect of M2 peptide on $\alpha_M\beta_2$-dependent adhesion to GP Ibα. 293 cells expressing $\alpha_M\beta_2$ were added to sGP Ibα–coated wells pre-incubated with 0–50 μM M2 (●) or scM2 (○) peptides. Adhesion was promoted by the addition of 5 μg/ml of the stimulating mAb KIM 127 and quantified by measuring the fluorescence of BCECF AM–loaded cells. Data represent mean ± SD, n = 3 independent experiments.

GP Ibα Binding to "Triple Mutants" of the $\alpha_M I$ Domain. To begin localization of specific amino acid residues within the α_MI domain involved in GP Ibα recognition, recombinant fragments containing wild-type α_MI domain, R^{115}–S^{340}, wild-type α_LI domain, P^{120}–S^{330}, and a mutant α_MI domain were expressed as GST fusion proteins in *Escherichia coli*. The mutant α_MI domain contained a swap of the P^{201}–K^{217} segment, which we implicated in sGP Ibα binding to the corresponding residues of the α_LI domain. The recombinant proteins were purified from the bacterial lysates on glutathione-Sepharose. A facile binding assay for quantifying sGP Ibα binding to the recombinant I domains was developed by measuring the binding of biotinylated sGP Ibα to the recombinant I domains immobilized onto 96-well plastic plates. As shown in Fig. 4, GP Ibα exhibited minimal reaction with α_LI domain. Binding was observed and was similar with both human and mouse α_MI domains. With the α_MI domains, binding was dependent on the sGP Ibα con-

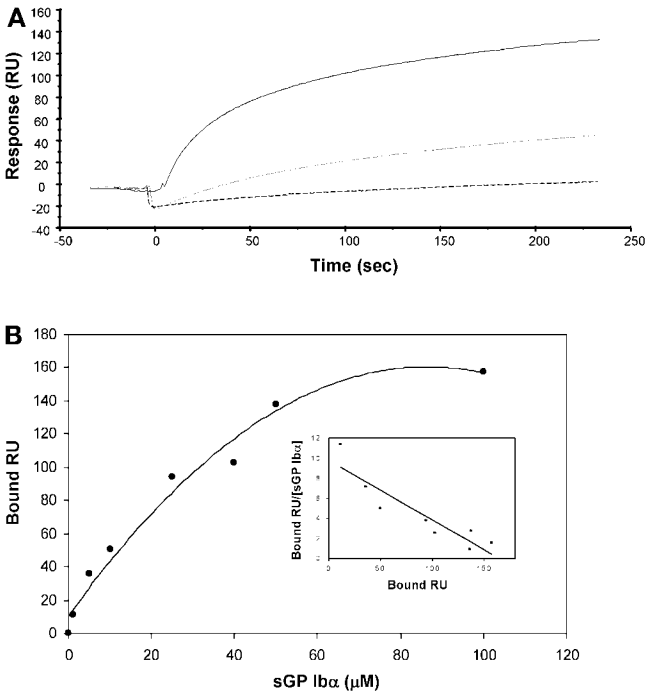

Figure 3. BIAcore analysis of the interaction between GP Ibα and M2. (A) 0–100 μM sGP Ibα in running buffer injected over control chips (dashed line) or chips immobilized with Cys-M2 (solid line) or Cys-scM2 (dotted line) for 4 min at a flow rate of 10 μl/min followed by running buffer alone. In all cases, sensograms obtained with control flow cells were subtracted from those obtained with immobilized peptides. (B) Plot of RU as a function of GP Ibα concentration. The inset shows Scatchard analysis to obtain apparent equilibrium dissociation constant (kD = 17 μM). RU, resonance unit.

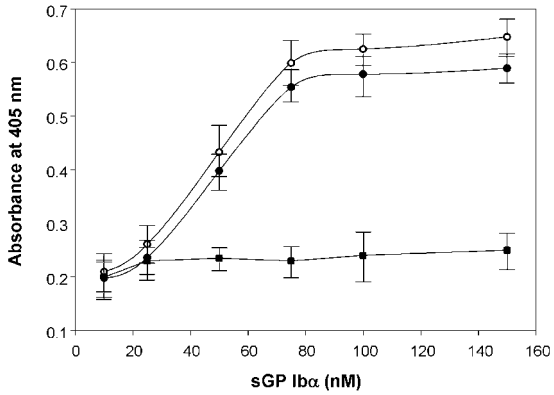

Figure 4. GP Ibα binding to recombinant I domains. Biotinylated sGP Ibα was added at the indicated concentrations to α_MI domain GST fusion proteins immobilized on microtiter wells. The various I domains are: human α_MI domain (○), mouse α_MI domain (●), and the α_LI domain (■). Incubations were performed in the presence of 2 mM Ca^{2+}, and samples were processed as indicated in Materials and Methods. Each dataset is the mean ± SEM of at least three independent experiments.

centration with 50% maximal binding observed at 50 nM sGP Ibα, which was used in subsequent experiments. As shown in Fig. 5 A, the interaction of the α_MI domain "swap" mutant with biotinylated sGP Ibα was greatly diminished compared with wild-type α_MI domain and similar to that of the α_LI domain. Essentially, no specific binding of sGP Ibα to this mutant I domain was detected. This result is consistent with our BIAcore binding experiments showing a direct interaction between sGP Ibα and immobilized M2 peptide corresponding to this P^{201}–K^{217} segment.

To begin to identify the individual residues within the P^{201}–K^{217} segment that mediated sGP Ibα recognition, a series of six triple mutants were created. In each of these triple mutants, a set of three consecutive amino acids within the α_MI domain was changed to the corresponding α_L residues. If the α_M and α_L residues were the same, the amino acid was mutated to alanine. After the DNA sequence of each mutant I domain was confirmed, it was expressed in *E. coli* and purified on glutathione-Sepharose. When analyzed by SDS-PAGE, each mutant migrated as a single band of ~52 kD (not depicted). sGP Ibα binding to each triple mutant was then assessed. The results in Fig. 5 A show the binding of each of the six triple mutants to 50 nM biotinylated sGP Ibα. Of the six triple mutants, three, H^{210}–A^{212}, T^{213}–I^{215}, and R^{216}–K^{217}, showed a significant reduction in sGP Ibα binding. Three mutants, P^{201}–T^{203}, Q^{204}–L^{206}, and G^{207}–T^{209}, did not impair binding to GP Ibα. These results, taken in light of the observation that mutating the entire region spanning P^{201}–G^{207} abolished cell adhesion to sGP Ibα (Fig. 1), suggest that the inactivation of sGP Ibα binding requires alteration of more than one residue within the P^{201}–G^{207} (i.e., no single residue within the triple mutants, P^{201}–T^{203}, Q^{204}–L^{206}, and G^{207}–T^{209}, decreases affinity detectably), or the conformation of the P^{201}–G^{207} segment, which corresponds to a portion of a loop within the α_MI domain, is necessary for binding, and, again, no single substitution alters the conformation of this region sufficiently to prevent binding.

GP Ibα Binding to "Single Point Mutants" of the α_MI Domain. Next, within the three triple mutants with reduced sGP Ibα binding, each of the three amino acids was mutated individually to the corresponding residue in α_LI domain or in case of identical residues in two I domains, the amino acid was replaced with an alanine. After confirming the DNA sequences of these single mutants, each of the GST fusion proteins was purified. The mutant fusion protein carrying the K^{217}Y substitution was insoluble. Therefore, K^{217} was mutated to Ala, and this α_MI domain with a K^{217}A substitution was readily purified, yielding a total of eight single mutants. The capacity of the eight single mutants to bind sGP Ibα is summarized in Fig. 5 B. Within each of the three triple mutants with reduced sGP Ibα recognition, only one of the three single mutants exhibited reduced sGP Ibα binding. These three single mutants showing reduced binding were T^{211}A, T^{213}G, and R^{216}N.

Development of a Chimeric α_LI Domain with GP Ibα Binding Activity. Loss of GP Ibα binding function in these single mutants could reflect direct involvement of the specific residues in GP Ibα binding or conformational perturbation of the resulting α_MI domain due to substitutions at these positions. A gain in function approach was used to distinguish between these possibilities by introducing the identi-

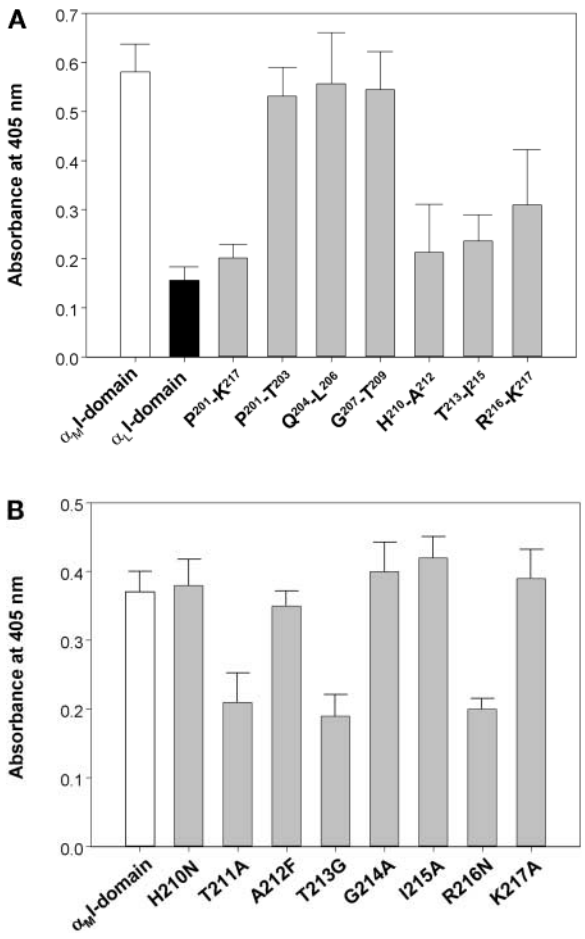

Figure 5. GP Ibα binding to α_MI domain triple mutants (A) and α_MI domain single mutants (B). The GST fusion proteins were adsorbed onto wells of microtiter plates, and sGP Ibα binding was measured using a 50-nM concentration of ligand. Each dataset is the mean ± SEM of at least three independent experiments.

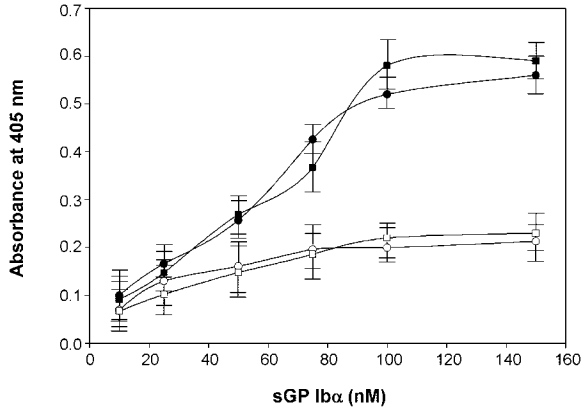

Figure 6. GP Ibα binding to the chimeric α_LI domain. Biotinylated sGP Ibα binding was measured as in Fig. 1 to wild-type α_MI domain (●), the α_LI domain (□), the chimeric α_LI domain (○) containing the single G(213)T mutation, and the chimeric α_LI domain containing the double $G^{213}T$ and $N^{216}R$ substitutions (■). Values are presented as the mean ± SEM of at least three separate experiments.

fied point mutations into the α_LI domain. T^{211} is conserved in both α_MI and α_LI domains. Therefore, chimeric I domains containing either a single $G^{213}T$ substitution or two substitutions, $G^{213}T$ and $N^{216}R$, in the α_LI domain backbone were created. These mutant α_LI domains were expressed as GST fusion proteins, purified, and their sGP Ibα binding properties were evaluated. The chimeric I domain harboring both the $G^{213}T$ and $N^{216}R$ mutations bound sGP Ibα with an affinity substantially greater than wild-type α_LI domain and the I domain containing the single $G^{213}T$ mutation (Fig. 6). Indeed, the binding capability of double substituted chimeric I domain was comparable to the wild-type α_MI domain. To confirm that these two amino acid residues are sufficient to impart sGP Ibα recognition to the mutated α_LI domain, we performed additional BIAcore binding assays with immobilized α_LI domain peptide (C^{201}HVKHMLLTNTFGAINY^{217}, termed C-L2) corresponding to the P^{201}–K^{217} sequence within α_MI domain and the double substituted mutant C^{201}HVKHMLLTNTFTAIRY^{217} (C-muL2). Binding assays were also performed with a mutant M2 peptide containing T^{211}A, T^{213}G, and R^{216}N substitutions (C^{201}PITQLLGRTHAAGGINK^{217}, termed C-muM2) corresponding to the three single mutants showing reduced binding in the purified mutant I domain binding assays (Fig. 5 B). The sensorgrams detected little interaction between 50 μM sGP Ibα and chips containing immobilized C-L2 (RU = 10) or C-muM2 (RU = 25). Significant interaction responses were detected for sGP Ibα with C-muL2 (RU = 224).

Role of the Identified Amino Acids in the Context of Intact $\alpha_M\beta_2$. The role of T^{213} and R^{216} in the GP Ibα binding function of the intact receptor was investigated. The $T^{213}G$ and $R^{216}N$ substitutions were introduced into the cDNA for the α_L subunit using site-directed mutagenesis and coexpressed with the cDNA for the β_2 subunit in 293 cells. Wild-type $\alpha_L\beta_2$ and $\alpha_M\beta_2$ were also transiently expressed in these cells as controls. 48 h after transfection, the cells were detached from tissue culture plates, and receptor expression levels were evaluated by FACS®. α_M expression was evaluated with OKM1, β_2 expression with IB4, and α_L expression with TS1/22. The expression levels of both the α and β subunits of the integrins were comparable (not depicted). Next, the function of the receptors was assessed by evaluating their adhesion to immobilized sGP Ibα. PMA, Mn^{2+}, or their combination were used to activate the integrins on the cells. As shown in Fig. 7, mock-transfected cells or cells expressing wild-type $\alpha_L\beta_2$ showed little adhesion to sGP Ibα under all conditions. When $\alpha_M\beta_2$-expressing cells were stimulated with PMA, Mn^{2+}, or their combination, their adhesion to sGP Ibα increased markedly compared with the nonstimulated cells. The chimeric $\alpha_L\beta_2$ cells adhered to sGP Ibα considerably better than the $\alpha_L\beta_2$ cells or mock-transfected cells. The adhesion of the chimeric $\alpha_L\beta_2$ cells approached that of the wild-type $\alpha_M\beta_2$ cells. We considered whether inserting these amino acid residues into α_L might affect the activation state of chimeric $\alpha_L\beta_2$ such that the increase in binding might reflect allosteric changes in the inte-

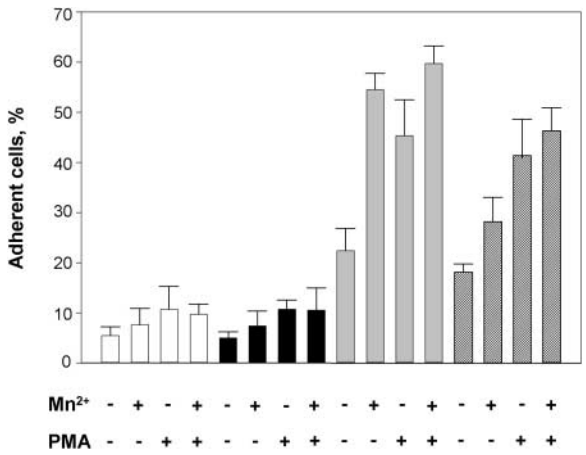

Figure 7. GP Ibα binding to the chimeric $\alpha_L\beta_2$. Adhesion of mock-transfected 293 cells (open bars), $\alpha_L\beta_2$-transfected cells (solid bars), $\alpha_M\beta_2$-transfected cells (gray bars), and cells expressing the chimeric $\alpha_L\beta_2$ receptor (striped bars) to sGP Ibα–coated wells. The percentage of input cells adherent after washing was calculated. Values are the mean ± SEM of three individual experiments.

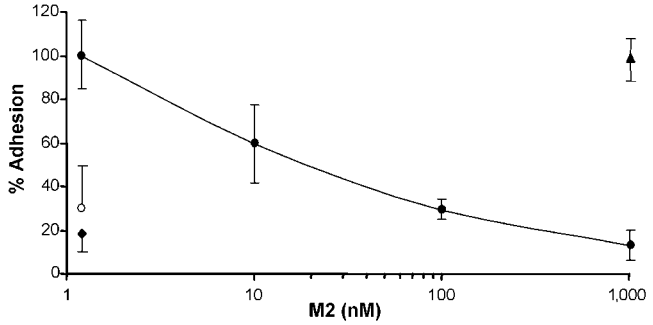

Figure 8. Neutrophil binding to platelets is inhibited by M2 peptide. Neutrophils from wild-type (Mac-$1^{+/+}$) or Mac-1–deficient (Mac-$1^{-/-}$, ◆) mice were added to surface-adherent platelets. Adhesion was promoted by the addition of 17 ng/ml PMA. The contribution of $\alpha_M\beta_2$ to wild-type neutrophil adhesion to platelets was also assayed by the addition of 10 μg/ml rat anti–mouse α_M mAb M1/70 (○). The effect of 0–1,000 nM M2 (●) and scM2 (▲) on neutrophil adhesion was also examined. Adhesion was quantified by measuring the fluorescence of BCECF AM–loaded neutrophils. Data are expressed as percent wild-type neutrophil adhesion with vehicle alone (mean ± SD, $n = 3$ independent experiments).

grin. Accordingly, we assessed the activation states of the chimeric integrin using MEM-83, an mAb that reacts with activated $\alpha_L\beta_2$ (33). In FACS® analyses, MEM-83 failed to react with either the $\alpha_L\beta_2$ or the chimeric $\alpha_L\beta_2$ transfectants in the unstimulated state (MFI = 14 and 10, respectively), but reacted well and equivalently with both transfectants upon stimulation with the combination of Mn^{2+} and PMA (MFI = 79 and 83, respectively). Thus, the activation states of both the $\alpha_L\beta_2$ and chimeric $\alpha_L\beta_2$ transfectants, with and without stimulation, were similar.

$\alpha_M\beta_2$ and GP Ibα Facilitate the Interaction between Leukocytes and Platelets. Having previously reported that $\alpha_M\beta_2$ and GP Ibα facilitate the heterotypic interaction between leukocytes and platelets, we turned to examining the effect of M2 on neutrophil adhesion to platelets. Thioglycollate-elicited neutrophils were added to wells containing surface adherent platelets and adhesion was stimulated by the addition of PMA to each well. We verified by FACS® analysis that such PMA treatment up-regulated P-selectin expression 29.9-fold in platelets purified and prepared with PGE1 as described in Materials and Methods. Wild-type (Mac-$1^{+/+}$) neutrophils bound to adherent platelets (Fig. 8). In contrast, Mac-1–deficient (Mac-$1^{-/-}$) neutrophils demonstrated markedly reduced adhesion to platelets (percent wild-type adhesion = 18.2 ± 8.0) and adhesion of wild-type neutrophils was blocked by the rat anti–mouse $\alpha_M\beta_2$ mAb M1/70 (percent wild-type adhesion = 29.9 ± 19.8), indicating that under these conditions, neutrophil adhesion to platelets is largely $\alpha_M\beta_2$ dependent, although a complimentary role for P-selectin/PSGL-1 is likely operative. M2, but not a scrambled version, inhibited dose dependently (IC_{50} = 30 nM) wild-type neutrophil adhesion to platelets. Taken together, these observations indicate that under these experimental conditions, neutrophil adhesion to platelets is mediated primarily by the α_MI domain sequence P^{201}–K^{217}.

M2 Peptide Abrogates the Firm Adhesion of THP-1 Cells under Flow. To evaluate the potential for M2 to modulate the adhesion of blood cells under flow, we perfused THP-1 cells that express Mac-1 over coverslips coimmobilized with soluble P-selectin and GP Ibα using a parallel plate flow chamber system (0.75 dynes/cm^2). The number of rolling and arrested cells was quantified on five random fields after 3 min of perfusion. THP-1 cells rolled and arrested on coverslips cocoated with P-selectin and sGP Ibα and the number of rolling (control vs. scM2, $P > 0.05$) or arrested (control vs. scM2, $P > 0.05$) cells was unaffected by scM2 (Fig. 9 A). In contrast, M2 peptide inhibited THP-1 cell arrest, thereby increasing the number of rolling cells visualized. The effect of M2 on cell adhesion was similar to treatment with LPM19c, an anti-CD11b mAb that blocks $\alpha_M\beta_2$-dependent binding to sGP Ibα, thereby confirming the involvement of $\alpha_M\beta_2$ in cell adhesion. Both cell rolling and arrest were abolished by treating cells with KPL-1, an anti–PSGL-1 mAb that blocks P-selectin binding. The effect of M2 on cell arrest was also quantified. Thus, on coverslips incubated with vehicle or scM2, 64 and 66% of THP-1 cells arrested, respectively (Fig. 9 B). After treatment with M2 peptide only 34% of cells arrested ($P < 0.05$). Similarly, after preincubation of THP-1 cells with LPM19C, only 33% of cells arrested ($P < 0.05$). KPL-1 antibody treatment abrogated almost all rolling and subsequent arrest (<10%; $P < 0.01$).

Discussion

In this study, we have identified the P^{201}–K^{217} segment, which spans an exposed loop and amphipathic α4 helix in the three-dimensional structure of the α_MI domain, as the binding site for platelet GP Ibα. This conclusion is supported by the following data: (a) mutant cell lines in which the α_MI domain segments P^{201}–G^{207} and R^{208}–K^{217} were

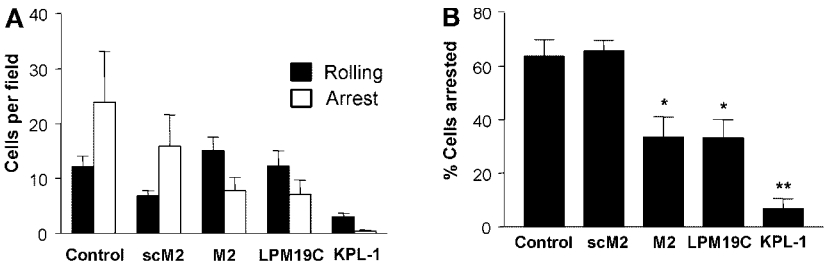

Figure 9. THP-1 cell adhesion under flow is inhibited by M2 peptide. Soluble GP Ibα was coimmobilized with P-selectin on coverslips. 0.6×10^6/ml THP-1 cells were activated with KIM 127 and drawn across the substrates at 0.75 dynes/cm^2 as detailed in Materials and Methods. The effect of M2 and scM2 peptides on THP-1 cell rolling and firm arrest was examined by preincubating 50 μM of the peptide with the ligand-coated coverslip. To block PSGL-1 and $\alpha_M\beta_2$ interactions, THP-1 cells were incubated with 20 μg/ml KPL-1 or LPM19c mAb, respectively, for 20 min before perfusion. The absolute number of rolling and arrested cells was quantified per ×10 field on five random fields after 3 min of perfusion. Data represent the mean ± SEM, $n = 3$ independent experiments. *, $P < 0.05$ versus control peptide; **, $P < 0.01$ versus control peptide.

switched to the homologous α_LI domain segments failed to support adhesion to sGP Ibα, (b) mutation of amino acid residues within P^{201}–K^{217}, H^{210}–A^{212}, T^{213}–I^{215}, and R^{216}–K^{217} resulted in the loss of the binding function of the recombinant α_MI domains to biotinylated sGP Ibα, (c) synthetic peptides duplicating the P^{201}–K^{217}, but not scrambled versions, directly bound sGP Ibα and inhibited $\alpha_M\beta_2$-dependent adhesion to sGP Ibα and adherent platelets, and (d) grafting key amino acids within the P^{201}–K^{217} sequence onto α_L converted $\alpha_L\beta_2$ into a GP Ibα binding integrin.

By virtue of binding diverse ligands including, among others, fibrin(ogen) (34, 35), ICAM-1 (36), factor X (37), C3bi (34), high molecular weight kininogen (38), and heparin (4), $\alpha_M\beta_2$ regulates important leukocyte functions including adhesion, migration, coagulation, proteolysis, phagocytosis, oxidative burst, and signaling (30, 39–42). However, these ligands do not account for all of $\alpha_M\beta_2$'s adhesive interactions. Although previous studies have shown that $\alpha_M\beta_2$ directly facilitates the recruitment of leukocytes at sites of platelet and fibrin deposition (5), the precise platelet counter receptors, including GP Ibα (11) and JAM-3 (43), have been elucidated only recently.

In this study, we have identified key elements of the binding site for GP Ibα within the α_MI domain. The strategy to define the ligand binding site was based on the difference in the sGP Ibα binding properties of the α_MI and α_LI domains and entailed four complimentary approaches. In the first approach, a series of homologue-scanning mutants, used previously to map the binding regions for NIF, iC3b, and fibrinogen (16, 20, 23), were screened for adhesion to sGP Ibα. In these mutants, 16 segments at the hydrated surface of the α_MI domain were replaced with the corresponding segments from the homologous α_LI domain, which does not bind GP Ibα. 11 mutants lacked the ability to support adhesion sGP Ibα, and alteration of two other regions, $\alpha_M(E^{178}$–$T^{185})$ and $\alpha_M(\Delta E^{262}G^{263})$, resulted in the partial loss of adhesive function. Thus, the initial insight provided by these mutant receptors indicated that the sGP Ibα binding interface within the α_MI domain was composed of several nonlinear sequences.

The second approach entailed the use of synthetic peptides duplicating the sequences of the critical segments in the α_M I domain. These analyses showed that two critical segments, $\alpha_M(P^{201}$–$G^{207})$ and $\alpha_M(R^{208}$–$K^{217})$, may contain amino acid residues that participate directly in binding GP Ibα because the peptide M2 that spanned P^{201}–K^{217} bound sGP Ibα and inhibited $\alpha_M\beta_2$-dependent adhesion to sGP Ibα and adherent platelets. The negative results for other peptides (M1, M3–M5, and M7) synthesized to correspond to other negative mutants (Fig. 1 and Table I) do not exclude a role for other α_MI domain segments in binding function. These segments may play an accessory role in ligand binding or the short peptides may simply not assume the appropriate conformation for recognition by the ligand. Finally, segments implicated in the binding of sGP Ibα by the negative mutants, other than P^{201}–K^{217}, may reflect interference by α_LI domain residues rather than residues that actually participate in binding. It is also possible that the activation of $\alpha_M\beta_2$, rather than ligand binding per se, was affected adversely by the introduction of these α_L segments within α_MI domain. Because these same mutants have been used in previous studies (17, 20, 23) to analyze interaction of other activation-dependent ligands with $\alpha_M\beta_2$, such effects on activation would need to specifically perturb GP Ibα recognition.

To obtain direct evidence that the $\alpha_M(P^{201}$–$K^{217})$ sequence constitutes the functional binding site for the GP Ibα, we turned to a third approach using site-directed mutagenesis of the α_MI domain. Binding experiments with purified sGP Ibα and GST-I domain mutants provided the independent confirmation that the P^{201}–K^{217} segment is important for sGP Ibα binding because mutations of these residues resulted in significant loss of sGP Ibα binding. These experiments also served to narrow further the binding region to H^{210}–K^{217} and subsequently identified three single mutants showing reduced binding to sGP Ibα (T^{211}A, T^{213}G, and R^{216}N). Of these, T^{211} in α_MI domain is conserved in the α_LI domain. Thus, it was the conversion of the residue to A that perturbed GP Ibα binding, suggesting that this substitution exerts a negative influence on the conformation of the α_MI domain that is required for GP Ibα recognition, rather than participating directly in ligand contact. The positioning of this residue on the interior of the α4-helix and facing the central core of the α_MI domain, according to the crystal structures (8, 9), supports this interpretation. In contrast, T^{213} and R^{216} are appropriately positioned, including when the recent crystal structure of the GP Ibα/vWF A domain (44) is used as a template.

In the fourth approach, the two amino acids (T^{213}G and R^{216}N substitutions) within the $\alpha_M(P^{201}$–$K^{217})$ were grafted

into the corresponding positions of the α_LI domain in the context of intact $\alpha_L\beta_2$. As demonstrated in Figs. 6 and 7, this manipulation imparted GP Ibα binding capacity to the chimeric molecule. Thus, the role of amino acids within the $\alpha_M(P^{201}–K^{217})$ sequence in GP Ibα binding, which initially was inferred from the loss in function experiments, was verified by the gain in function approach. Taken together, the four approaches substantiated independently the role of $\alpha_M(P^{201}–K^{217})$ in GP Ibα binding and provided evidence that two to three critical residues participate in ligand docking.

To date, several lines of evidence have emphasized that multiple ligands share overlapping binding sites within $\alpha_M\beta_2$, including the fact that one ligand (e.g., NIF) is capable of blocking the interaction of multiple ligands (C3bi, ICAM-1, fibrinogen) with the receptor (15, 45). However, although the binding sites for these ligands might be overlapping, they need not be identical (16, 17). Ustinov and Plow (22) have proposed a mosaic model in which many of the same loops and helices of the α_MI domain, on or near its MIDAS face, may engage ligands, but different amino acid residues within these structures may contact the ligands. Direct support for this mosaic model is seen within the $K^{245}–R^{261}$ segment of the α_MI domain, which has been implicated in both NIF and fibrinogen recognition (23). Key contact amino acids in this loop for fibrinogen binding are F^{246}, D^{254}, and P^{257}, whereas Y^{252} and E^{258} are involved in NIF binding. This same α_MI domain segment is also involved in C3bi recognition by $\alpha_M\beta_2$ (17).

Under the experimental conditions used in this study, which assayed the adhesion of activated neutrophils to surface-adherent platelets after vigorous washing, the predominant interaction between neutrophils and platelets appeared to be mediated by $\alpha_M\beta_2$ binding to sGP Ibα, based on the ability of M2 to inhibit >80% of neutrophil adhesion. The enhanced potency of M2 with respect to inhibiting neutrophil adhesion to platelets (IC_{50} = 30 nM) compared with BIAcore (kD = 17 μM) is possibly secondary to the fact that leukocytes express $\alpha_M\beta_2$ and platelets express GP Ibα in their native conformations. In contrast, BIAcore experiments used sGPIbα with immobilized M2 peptide.

Our data do not rule out the possibility of additional platelet surface receptors for $\alpha_M\beta_2$. Other potential $\alpha_M\beta_2$ ligands present on the platelet membrane include fibrinogen (bound to GP IIb-IIIa; 34, 35), ICAM-2 (46), high molecular weight kininogen (38), and JAM-3 (43). However, a leukocyte–platelet interaction mediated by fibrinogen bridging between $\alpha_M\beta_2$ and GP IIb/IIIa has been discounted by Ostrovsky et al. (47), who found that neither RGDS peptides nor the replacement of normal platelets with thrombasthenic platelets (i.e., lacking GP IIb/IIIa) affected the accumulation of the leukocytes on platelets. Although $\alpha_M\beta_2$ binds ICAM-1, this receptor is not found on platelets. Platelets express a related receptor, ICAM-2 (48), but Diacovo et al. (5) have shown that ICAM-2 blockade has no effect on the firm adhesion of neutrophils on monolayers of activated platelets under flow. Santoso et al. (43) have reported recently that $\alpha_M\beta_2$ may also bind to platelet JAM-3, cooperating with GP Ibα to mediate neutrophil–platelet adhesive contacts (43).

The present observations also suggest a possible target for therapeutic intervention. In particular, the specificity of M2 inhibitory action toward GP Ibα (i.e., noninhibitory toward fibrinogen) suggests that it might be possible to prevent leukocyte attachment to platelets by targeting GP Ibα without inhibiting other $\alpha_M\beta_2$ functions. Our recent observations have identified $\alpha_M\beta_2$ as a molecular determinant of neointimal thickening after experimental arterial injury that produces endothelial denudation and platelet deposition. We found that antibody-mediated blockade (49) or selective absence (50) of $\alpha_M\beta_2$ impaired transplatelet leukocyte migration into the vessel wall, diminishing medial leukocyte accumulation and neointimal thickening after experimental angioplasty or endovascular stent implantation. Therefore, this study identifying the precise binding site responsible for $\alpha_M\beta_2$–GP Ibα interaction might provide a molecular strategy for disrupting leukocyte–platelet complexes that promote vascular inflammation in thrombosis, atherosclerosis, and angioplasty-related restenosis.

This work was supported in part by grants from the National Institutes of Health (HL53993, HL36028, and HL65090 to F.W. Luscinskas, HL65967 and HL64796 to J.A. Lopez, HL66197 to E.F. Plow, and HL57506 and HL60942 to D.I. Simon). R. Ehlers received a post-doctoral research fellowship from Society for Thrombosis and Hemostasis Research, Germany. V. Ustinov received a post-doctoral research fellowship from The Ohio Valley Affiliate, American Heart Association (0120394B). R.M. Rao is an ARC Copeman Traveling Research Fellow.

Note added in proof. Hoffmeister et al. (Hoffmeister, K.M., E.C. Josefsson, N.A. Isaac, H. Clausen, J.H. Hartwig, and T.P. Stossel. 2003. Glycosylation restores survival of chilled blood platelets. *Science.* 301: 1531–1534.) have recently reported that chilled platelets are cleared by hepatic macrophage $\alpha_M\beta_2$ receptors via an interaction between platelet GP Iβα and a non–I-domain, lectin-binding site within $a_M\beta_2$.

Submitted: 20 December 2002
Revised: 6 August 2003
Accepted: 12 August 2003

References

1. Springer, T.A. 1994. Traffic signals for lymphocyte recirculation and leukocyte emigration: a multistep paradigm. *Cell.* 76:301–314.
2. Smith, C.W., S.D. Marlin, R. Rothlein, C. Toman, and D.C. Anderson. 1989. Cooperative interactions of LFA-1 and Mac-1 with intercellular adhesion molecule-1 in facilitating adherence and transendothelial migration of human neutrophils in vitro. *J. Clin. Invest.* 83:2008–2017.
3. Languino, L.R., A. Duperray, K.J. Joganic, M. Fornaro, G.B. Thornton, and D.C. Altieri. 1995. Regulation of leukocyte-endothelium interaction and leukocyte transendothelial migration by intercellular adhesion molecule 1-fibrinogen recognition. *Proc. Natl. Acad. Sci. USA.* 92:1505–1509.
4. Diamond, M.S., R. Alon, C.A. Parkos, M.T. Quinn, and T.A. Springer. 1995. Heparin is an adhesive ligand for the leukocyte integrin Mac-1 (CD11b/CD18). *J. Cell Biol.* 130:1473–1482.
5. Diacovo, T.G., S.J. Roth, J.M. Buccola, D.F. Bainton, and

T.A. Springer. 1996. Neutrophil rolling, arrest, and transmigration across activated, surface-adherent platelets via sequential action of P-selectin and the beta 2-integrin CD11b/CD18. *Blood*. 88:146–157.
6. McEver, R.P., and R.D. Cummings. 1997. Role of PSGL-1 binding to selectins in leukocyte recruitment. *J. Clin. Invest.* 100:S97–S103.
7. Diamond, M.S., J. Garcia-Aguilar, J.K. Bickford, A.L. Corbi, and T.A. Springer. 1993. The I domain is a major recognition site on the leukocyte integrin Mac-1 (CD11b/CD18) for four distinct adhesion ligands. *J. Cell Biol.* 120:1031–1043.
8. Lee, J.O., P. Rieu, M.A. Arnaout, and R. Liddington. 1995. Crystal structure of the A domain from the alpha subunit of integrin CR3 (CD11b/CD18). *Cell.* 80:631–638.
9. Qu, A., and D.J. Leahy. 1995. Crystal structure of the I-domain from the CD11a/CD18 (LFA-1, alpha L beta 2) integrin. *Proc. Natl. Acad. Sci. USA* 92:10277-10281.
10. Sadler, J.E., B.B. Shelton-Inloes, J.M. Sorace, J.M. Harlan, K. Titanti, and E.W. Davie. 1985. Cloning and characterization of two cDNAs coding for human von Willebrand factor. *Proc. Natl. Acad. Sci. USA*. 82:6394–6398.
11. Simon, D.I., Z. Chen, H. Xu, C.Q. Li, J. Dong, L.V. McIntire, C.M. Ballantyne, L. Zhang, M.I. Furman, M.C. Berndt, et al. 2000. Platelet glycoprotein Ibα is a counterreceptor for the leukocyte integrin Mac-1 (CD11b/CD18). *J. Exp. Med.* 192:193–204.
12. Diamond, M., J. Garcia-Aguiliar, J. Bickford, A. Corbi, and T. Springer. 1993. The I domain is a major recognition site on the leukocyte integrin Mac-1 (CD11b/CD18) for four distinct ligands. *J. Cell Biol.* 120:1031–1043.
13. Zhou, L., D.H. Lee, J. Plescia, C.Y. Lau, and D.C. Altieri. 1994. Differential ligand binding specificities of recombinant CD11b/CD18 integrin I-domain. *J. Biol. Chem.* 269:17075–17079.
14. Ueda, T., P. Rieu, J. Brayer, and M.A. Arnaout. 1994. Identification of the complement iC3b binding site in the beta 2 integrin CR3 (CD11b/CD18). *Proc. Natl. Acad. Sci. USA*. 91:10680–10684.
15. Rieu, P., T. Ueda, I. Haruta, C.P. Sharma, and M.A. Arnaout. 1994. The A-domain of beta 2 integrin CR3 (CD11b/CD18) is a receptor for the hookworm-derived neutrophil adhesion inhibitor NIF. *J. Cell Biol.* 127:2081–2091.
16. Zhang, L., and E.F. Plow. 1996. A discrete site modulates activation of I domains. *J. Biol. Chem.* 271:29953–29957.
17. Zhang, L., and E.F. Plow. 1999. Amino acid sequences within the alpha subunit of integrin alpha M beta 2 (Mac-1) critical for specific recognition of C3bi. *Biochemistry*. 38: 8064–8071.
18. Rieu, P., T. Sugimori, D.L. Griffith, and M.A. Arnaout. 1996. Solvent-accessible residues on the metal ion-dependent adhesion site face of integrin CR3 mediate its binding to the neutrophil inhibitory factor. *J. Biol. Chem.* 271:15858–15861.
19. McGuire, S.L., and M.L. Bajt. 1995. Distinct ligand binding sites in the I domain of integrin alpha M beta 2 that differentially affect a divalent cation-dependent conformation. *J. Biol. Chem.* 270:25866–25871.
20. Zhang, L., and E.F. Plow. 1997. Identification and reconstruction of the binding site within αMβ2 for a specific and high affinity ligand, NIF. *J. Biol. Chem.* 272:17558–17564.
21. Li, R., P. Rieu, D.L. Griffith, D. Scott, and M.A. Arnaout. 1998. Two functional states of the CD11b A-domain: correlations with key features of two Mn^{2+}-complexed crystal structures. *J. Cell Biol.* 143:1523–1534.
22. Ustinov, V.A., and E.F. Plow. 2002. Delineation of the key amino acids involved in neutrophil inhibitory factor binding to the I-domain supports a mosaic model for the capacity of integrin alphaMbeta 2 to recognize multiple ligands. *J. Biol. Chem.* 277:18769–18776.
23. Yakubenko, V.P., D.A. Solovjov, L. Zhang, V.C. Yee, E.F. Plow, and T.P. Ugarova. 2001. Identification of the binding site for fibrinogen recognition peptide gamma 383-395 within the alpha MI-domain of integrin alpha Mbeta 2. *J. Biol. Chem.* 276:13995–14003.
24. Ault, K.A., and T.A. Springer. 1981. Cross-reaction of a rat-anti-mouse phagocyte-specific monoclonal antibody (anti-Mac-1) with human monocytes and natural killer cells. *J. Immunol.* 120:359–364.
25. Diamond, M.S., and T.A. Springer. 1993. A subpopulation of Mac-1 (CD11b/CD18) molecules mediates neutrophil adhesion to ICAM-1 and fibrinogen. *J. Cell Biol.* 120:545–556.
26. Robinson, M.K., D. Andrew, H. Rosen, D. Brown, S. Ortlepp, P. Stephens, and E.C. Butcher. 1982. Antibody directed against the Leu-CAM b-chain (CD18) promotes both LFA-1- and CR3-dependent adhesion events. *J. Immunol.* 148:1080–1085.
27. Dransfield, I., and N. Hogg. 1989. Regulated expression of Mg2+ binding epitope on leukocyte integrin alpha subunits. *EMBO J.* 8:3759–3765.
28. Simon, D.I., N.K. Rao, H. Xu, Y. Wei, O. Majdic, E. Ronne, L. Kobzik, and H.A. Chapman. 1996. Mac-1 (CD11b/CD18) and the urokinase receptor (CD87) form a functional unit on monocytic cells. *Blood*. 88:3185–3194.
29. Zhang, L., and E.F. Plow. 1996. Overlapping, but not identical, sites are involved in the recognition of C3bi, neutrophil inhibitory factor, and adhesive ligands by the alphaMbeta2 integrin. *J. Biol. Chem.* 271:18211–18216.
30. Lu, H., C.W. Smith, J. Perrard, D. Bullard, L. Tang, S.B. Shappell, M.L. Entman, A.L. Beaudet, and C.M. Ballantyne. 1997. LFA-1 is sufficient in mediating neutrophil emigration in Mac-1-deficient mice. *J. Clin. Invest.* 99:1340–1350.
31. Dallacqua, W., E.R. Goldman, E. Eisenstein, and R.A. Mariuzza. 1996. A mutational analysis of the binding of two different proteins to the same antibody. *Biochemistry*. 35:9667–9676.
32. Luscinskas, F.W., G.S. Kansas, H. Ding, P. Pizcueta, B.E. Schleiffenbaum, T.F. Tedder, and M.A. Gimbrone, Jr. 1994. Monocyte rolling, arrest and spreading on IL-4–activated vascular endothelium under flow is mediated via sequential action of L-selectin, β 1-integrins, and β 2-integrins. *J. Cell Biol.* 125:1417–1427.
33. Landis, R.C., A. McDowall, C.L. Holness, A.J. Littler, D.L. Simmons, and N. Hogg. 1994. Involvement of the "I" domain of LFA-1 in selective binding to ligands ICAM-1 and ICAM-3. *J. Cell Biol.* 126:529–537.
34. Wright, S.D., J.S. Weitz, A.J. Huang, S.M. Levin, S.C. Silverstein, and J.D. Loike. 1988. Complement receptor type three (CD11b/CD18) of human polymorphonuclear leukocytes recognizes fibrinogen. *Proc. Natl. Acad. Sci. USA*. 85: 7734–7738.
35. Altieri, D.C., R. Bader, P.M. Mannucci, and T.S. Edgington. 1988. Oligospecificity of the cellular adhesion receptor Mac-1 encompasses an inducible recognition specificity for fibrinogen. *J. Cell Biol.* 107:1893–1900.

36. Diamond, M.S., D.E. Staunton, S.D. Marlin, and T.A. Springer. 1991. Binding of the integrin Mac-1 (CD11b/CD18) to the third immunoglobulin-like domain of ICAM-1 (CD54) and its regulation by glycosylation. *Cell.* 65:961–971.
37. Altieri, D.C., J.H. Morrissey, and T.S. Edgington. 1988. Adhesive receptor Mac-1 coordinates the activation of factor X on stimulated cells of monocytic and myeloid differentiation: an alternative initiation of the coagulation cascade. *Proc. Natl. Acad. Sci. USA.* 85:7426–7466.
38. Wachtfogel, Y.T., R.A. DeLa Cadena, S.P. Kunapuli, L. Rick, M. Miller, R.L. Schultz, D.C. Altieri, T.S. Edgington, and R.W. Colman. 1994. High molecular weight kininogen binds to Mac-1 on neutrophils by its heavy chain (domain 3) and its light chain (domain 5). *J. Biol. Chem.* 269:19307–19312.
39. Arnaout, M.A. 1990. Leukocyte adhesion molecules deficiency: its structural basis, pathophysiology and implications for modulating the inflammatory response. *Immunol. Rev.* 114:145–180.
40. Plow, E.F., and L. Zhang. 1997. A MAC-1 attack: integrin functions directly challenged in knockout mice. *J. Clin. Invest.* 99:1145–1146.
41. Coxon, A., P. Rieu, F.J. Barkalow, S. Askari, A.H. Sharpe, U.H. von Andrian, M.A. Arnaout, and T.N. Mayadas. 1996. A novel role for the beta 2 integrin CD11b/CD18 in neutrophil apoptosis: a homeostatic mechanism in inflammation. *Immunity.* 5:653–666.
42. Shi, C., X. Zhang, Z. Chen, M.K. Robinson, and D.I. Simon. 2001. Leukocyte integrin Mac-1 recruits toll/interleukin-1 receptor superfamily signaling intermediates to modulate NF-kappaB activity. *Circ. Res.* 89:859–865.
43. Santoso, S., U.J. Sachs, H. Kroll, M. Linder, A. Ruf, K.T. Preissner, and T. Chavakis. 2002. The junctional adhesion molecule 3 (JAM-3) on human platelets is a counterreceptor for the leukocyte integrin Mac-1. *J. Exp. Med.* 196:679–691.
44. Huizinga, E.G., S. Tsuji, R.A. Romijn, M.E. Schiphorst, P.G. de Groot, J.J. Sixma, and P. Gros. 2002. Structures of glycoprotein Ibalpha and its complex with von Willebrand factor A1 domain. *Science.* 297:1176–1179.
45. Forsyth, C.B., E.F. Plow, and L. Zhang. 1998. Interaction of the fungal pathogen *Candida albicans* with integrin CD11b/CD18: recognition by the I domain is modulated by the lectin-like domain and the CD18 subunit. *J. Immunol.* 161: 6198–6205.
46. Xie, J., R. Li, P. Kotovuori, C. Vermot-Desroches, J. Wijdenes, M.A. Arnaout, P. Nortamo, and C.G. Gahmberg. 1995. Intercellular adhesion molecule-2 (CD102) binds to the leukocyte integrin CD11b/CD18 through the A domain. *J. Immunol.* 155:3619–3628.
47. Ostrovsky, L., A.J. King, S. Bond, D. Mitchell, D.E. Lorant, G.A. Zimmerman, R. Larsen, X.F. Niu, and P. Kubes. 1998. A juxtacrine mechanism for neutrophil adhesion on platelets involves platelet-activating factor and a selectin-dependent activation process. *Blood.* 91:3028–3036.
48. Diacovo, T.G., A.R. de Fougerolles, D.F. Bainton, and T.A. Springer. 1994. A functional integrin ligand on the surface of platelets: intercellular adhesion molecule-2. *J. Clin. Invest.* 94: 1243–1251.
49. Rogers, C., E.R. Edelman, and D.I. Simon. 1998. A monoclonal antibody to the β2-leukocyte integrin Mac-1 (CD11b/CD18) reduces intimal thickening after angioplasty or stent implantation in rabbits. *Proc. Natl. Acad. Sci. USA.* 95:10134–10139.
50. Simon, D.I., Z. Chen, P. Seifert, E.R. Edelman, C.M. Ballantyne, and C. Rogers. 2000. Decreased neointimal formation in Mac-1(−/−) mice reveals a role for inflammation in vascular repair after angioplasty. *J. Clin. Invest.* 105:293–300.
51. Hoffmeister, K.M., E.C. Josefsson, N.A. Isaac, H. Clausen, J.H. Hartwig, and T.P. Stossel. 2003. Glycosylation restores survival of chilled blood platelets. *Science.* 301:1531–1534.